

Self-assembled fractal hybrid dendrites from water-soluble anionic (thia)calix[4] arenes and Ag⁺

Luidmila S. Yakimova · Leysan H. Gilmanova ·
Vladimir G. Evtugyn · Yuri N. Osin · Ivan I. Stoikov 

Received: 8 February 2017 / Accepted: 21 April 2017 / Published online: 10 May 2017
© Springer Science+Business Media Dordrecht 2017

Abstract Novel water-soluble anionic *p*-*tert*-butylthiacalix[4]arene with propanesulfonate fragments has been synthesized. Alkylation of the lower rim of thiacalix[4]arene in the presence of NaH/THF led to *cone* conformation instead of the expected *1,3-alternate* conformer due to metal template effect. The presence of supramolecular associates at the critical micelle concentration of $1.65 \cdot 10^{-5}$ M were investigated in aqueous solutions by a combination of different techniques (DLS and conductivity). It was observed that the macrocyclic platform decreases the CMC by tenfold as compared with non-macrocyclic analogs. A simple approach for the design of stable monodisperse Ag-based nanoaggregates (near 95 nm) containing ionic Ag and organic ligand–thiacalix[4]arene sulfo derivative in water has been developed. Self-assembled fractal hybrid nanodendrites consisting of water-soluble anionic

(thia)calix[4]arenes and Ag⁺ have been obtained in a single step under mild conditions.

Keywords Self-assembly · Dendrite · (Thia)calix[4]arene · Ag-based aggregates · Electron microscopy · Mapping · Stable suspensions

Introduction

The synthesis of stable, concentrated aqueous dispersions with desired physicochemical properties on the basis of silver nanoparticles (Ag NPs) and various Ag-based aggregates containing ionic or metallic Ag is a necessary step in the preparation of nanostructural materials used in microelectronics, electrochemistry, in the synthesis of pigments for optoelectronic sensors, etc. (Ariga et al. 2012; Ariga et al. 2013; Hussain et al. 2003). Fractal hybrid dendrites are a type of nanostructural materials generally formed by self-assembly under far-from-equilibrium conditions; as such, self-assembly is a natural and spontaneous process (Witten and Sander 1981; Melnikau et al. 2013). The creation of fractal hybrid dendrites offers an opportunity for their application in diverse functions such as in catalysis (Mohanty et al. 2010), optics (Polshettiwar et al. 2009), sensor technology (Wen et al. 2006), and in information storage (Zhou et al. 2007), depending on their specific physical and chemical properties. Besides, Ag-based aggregates are often used to produce various materials with antibacterial properties (Landsdown 2010). Silver ions have a pronounced ability to inactivate viruses like smallpox and influenza A-1 and B. They are active against some enteroviruses,

Electronic supplementary material The online version of this article (doi:10.1007/s11051-017-3868-9) contains supplementary material, which is available to authorized users.

L. S. Yakimova · L. H. Gilmanova · I. I. Stoikov (✉)
A. M. Butlerov Chemical Institute, Kazan Federal University,
Kremlevskaya 18, Kazan, Russian Federation 420008
e-mail: ivan.stoikov@mail.ru

L. S. Yakimova
Organic Chemistry Department, Faculty of Science, RUDN
University, 6 Miklukho-Maklaya St, Moscow, Russian Federation
117198

V. G. Evtugyn · Y. N. Osin
Interdisciplinary Centre for Analytical Microscopy, Kazan Federal
University, Kremlevskaya 18, Kazan, Russian Federation 420008

adenovirus, and human immunodeficiency virus (HIV) (Galdiero et al. 2011; Mohammed et al. 2012). It has been observed that the effect of Ag-based compounds depends on their size, concentration, and dispersion stability (Chen et al. 2013). Thus, the synthesis of stable, low-diversity, water-soluble Ag-based aggregates have attracted the attention of researchers. The preparation of nanoparticles and nanomaterials with unique properties using non-covalent self-assembly of supramolecular systems is a rapidly evolving research area (Steed and Atwood 2009; Atwood and Steed 2008; Lindoy and Atkinson 2000; Fujita 2000). Such systems can be formed by noncovalent self-assembly of molecular building blocks, which are characterized by strictly defined size, shape, and their ability of multiple recognition (Boal et al. 2000). Compared to other macrocyclic platforms, thiacalix[4]arenes (Puplampu et al. 2015; Puplampu et al. 2014; Stoikov et al. 2010; Vavilova et al. 2013) have a special place in supramolecular chemistry as molecular building blocks (Yakimova et al. 2016a; Ziganshin et al. 2006; Gorbachuk et al. 2004; Yakimova et al. 2016b; Shurpik et al. 2015a; Shurpik et al. 2014; Shurpik et al. 2015b), due to the following: (1) the initial

macrocycles can be easily obtained by a one-step synthesis; (2) the template effect of alkali metal ions allows one to prepare four isomers of the substituted p-tert-butylthiacalix[4]arene: cone, partial cone, 1,2-alternate, and 1,3-alternate; (3) their sulfide bridged fragments can coordinate transition metal cations; (4) the upper and lower rims of the macrocycle can be modified by various functional groups.

In this paper, we report a new approach for the design of Ag-based aggregates containing ionic Ag and organic ligands, i.e., water-soluble p-tert-butyl(thia)calix[4]arenes bearing O-3-propanesulfonate fragments at the lower rim (Fig. 1b). A simple preparation technique for stable, monodisperse Ag-based aggregates in water is proposed.

Experimental

^1H NMR, ^{13}C , and 2D ^1H - ^1H NOESY spectra were recorded on the Bruker Avance-400 (400, 100 MHz, respectively) spectrometer. Chemical shifts were determined against the signals of residual protons of

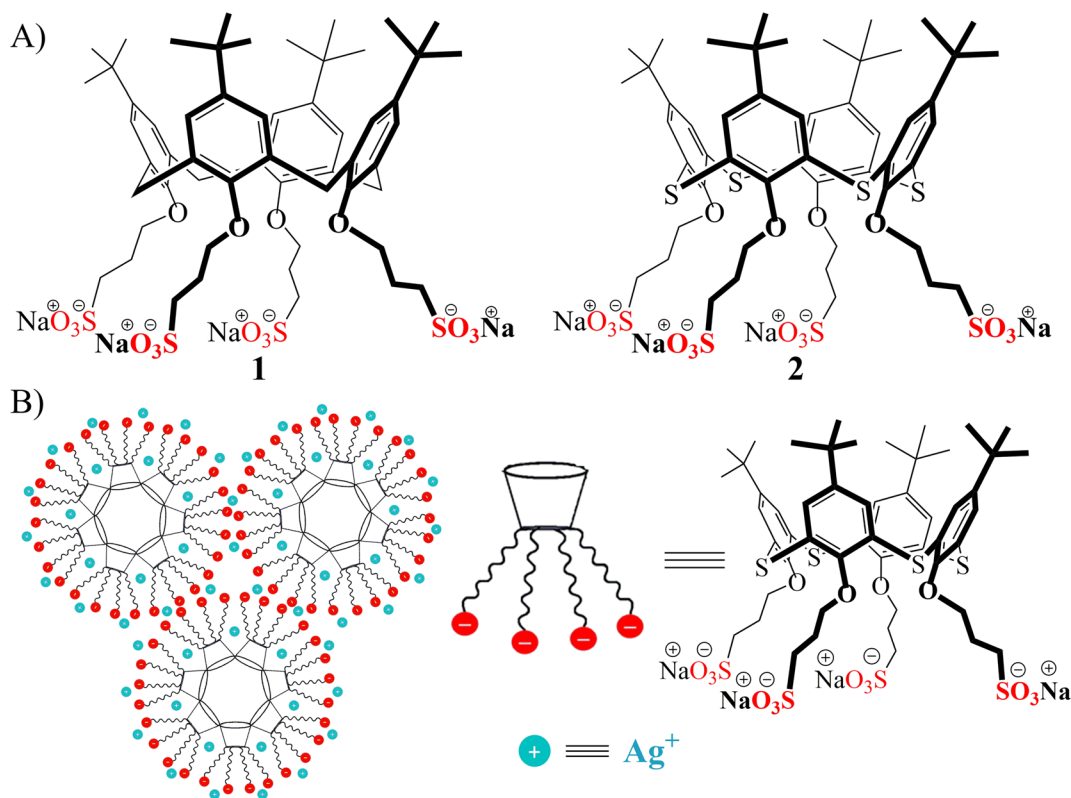


Fig. 1 a Structures of the (thia)calix[4]arenes **1** and **2**; b outline representation of the water-soluble thiacalix[4]arene **2** and of the formation of the thiacalix[4]arene stabilized silver nanoparticles

deuterated solvent (D₂O). The concentration of the sample solutions was equal to 3–5%. Attenuated total internal reflectance IR spectra were recorded with Spectrum 400 (Perkin Elmer) Fourier spectrometer. Elemental analysis was performed with Perkin Elmer 2400 Series II instrument. ESI mass spectra were recorded using mass spectrometer AmazonX (Bruker Daltonik GmbH, Germany). Negatively charged ions were registered within 100–2800 m/z. The voltage at the capillary was equal to –140 V. Nitrogen with the temperature of 300 °C and flow rate of 10 min⁻¹ was used as drying gas. Compounds were dissolved in acetonitrile to their concentration of 10⁻⁶ g/l. Data were processed using DataAnalysis 4.0 program (Bruker Daltonik GmbH, Germany). Melting points were determined using the Boetius Block apparatus. To determine the presence of sodium cations in aqueous solutions of thiacalixarene, ion chromatography ICS-5000 DIONEX was performed. Conductivity measurements were performed in water, with an InoLab Cond Level 1-720 conductometer equipped with a LR 325/001 immersion cell. Most chemicals were purchased from Aldrich and used as received without additional purification. Organic solvents were purified in accordance with standard procedures.

Synthesis

General method for synthesis of compounds 1, 2

NaH (60% in oil; 0.2 g, 7 mmol) was washed with absolute hexane and placed into the 100-ml round-bottom flask containing anhydrous THF and equipped with magnetic stirrer and reflux condenser. *p*-Tert-butylcalix[4]arene / *p*-tert-butylthiacalix[4]arene (0.6 mmol) was dissolved in a small amount of THF and added within 15 min to the reaction mixture. The reaction mixture was stirred at reflux temperature for 30 min. 1,3-Propanesultone (0.9 g, 7 mmol) was added to the reaction mixture and refluxed for 48 h. The product was filtered and washed with MeOH (3 × 10 ml), then recrystallized from acetone-water (10 ml), and filtered.

Sodium p-tert-butyl-calix[4]arenetetra-O-(3-propoxysulfonato) (1). Yield: 0.16 g (42%). M.p.: >350 °C. ¹H NMR (400 MHz, D₂O, 298 K), δ (ppm), *J*/Hz: 6.67 (s, 2H, ArH); 4.13, 2.97 AB system (2H, Ar-CH₂-Ar, ³*J*_{HH} = 12.6); 3.79 (t, 4H, –O–CH₂–, ³*J*_{HH} = 6.8); 2.85 (tt, 4H, –CH₂–CH₂–CH₂–,

³*J*_{HH} = 9.3); 2.09 (t, 4H, –CH₂–SO₃⁻, ³*J*_{HH} = 7.5); 0.78 (s, 6H, *t*-Bu). ¹³C NMR (100 MHz, D₂O, 298 K), δ (ppm): 25.35, 30.84, 33.76, 48.76, 60.15, 74.29, 129.68, 134.20, 146.55, 158.36. IR (ν/cm⁻¹): 1186.81 (SO₂), 1123.73, 1041.83 (S = O), 868.21, 794.59 (S–O), 590.41 (C–S). MS (ESI): calc. [M]⁻ m/z = 1201.4 M⁻¹, 589.2 M⁻², 385.1 M⁻³, 283.1 M⁻⁴, found [M]⁻ m/z = 1201.4 M⁻¹, 589.2 M⁻², 385.1 M⁻³, 283.6 M⁻⁴. Found (%): C, 54.82; H, 6.17; S, 10.39. Calc. (%): C, 54.89; H, 6.25; S, 10.47.

Sodium p-tert-butyl-thiacalix[4]arenetetra-O-(3-propoxysulfonato) (2). Yield: 0.07 g (36%). M.p.: >350 °C. ¹H NMR (400 MHz, D₂O, 298 K), δ (ppm), *J*/Hz: 7.32 (s, 2H, ArH); 4.28 (t, 4H, –O–CH₂–, ³*J*_{HH} = 6.2); 3.20 (t, 4H, –CH₂–SO₃⁻, ³*J*_{HH} = 6.9); 2.13 (tt, 4H, –CH₂–CH₂–CH₂–, ³*J*_{HH} = 6.97.5); 0.97 (s, 6H, *t*-Bu). ¹³C NMR (100 MHz, D₂O, 298 K), δ (ppm): 22.91, 28.81, 31.30, 46.26, 71.24, 122.99, 131.88, 142.89, 150.84. IR (ν/cm⁻¹): 1240.82, 1043.49 (S = O), 1180.70 (SO₂), 893.91 (S–O), 744 (C–S). MS (ESI): calc. [M]⁻ m/z = 1273.2 M⁻¹, 625.1 M⁻², 409.1 M⁻³, found [M]⁻ m/z = 1273.2 M⁻¹, 625.1 M⁻², 409.1 M⁻³. Found (%): C, 48.11; H, 5.25; S, 19.75. Calc. (%): C, 48.13; H, 5.28; S, 19.77.

Transmission electron microscopy

Transmission electron microscopy (TEM) analysis of NPs was carried out using the Hitachi HT7700 Exalens transmission electron microscope with Oxford Instruments X-Maxⁿ 80T EDS detector. For sample preparation, 10 μl of the suspension was placed on the FormvarTM/carbon-coated 3-mm copper grid, which was then dried at room temperature. After complete drying, the grid was placed into the transmission electron microscope using special holder for microanalysis. Analysis was held at the accelerating voltage of 80 kV in STEM mode using Oxford Instruments X-Maxⁿ 80T EDS detector.

Dynamic light scattering

The particle size was determined by the Zetasizer Nano ZS instrument at 20 °C. The instrument contains 4 mW He-Ne laser operating at a wavelength of 633 nm and incorporated noninvasive backscatter optics (NIBS). The measurements were performed at the detection angle of 173° and the software automatically determined the measurement position within the quartz cuvette. The

10^{-4} M aqueous solutions of **1**, **2** were prepared. The experiments were carried out for each solution in triplicate. The synthesized *p-tert*-butyl(thia)calix[4]arenes **1**, **2** dissolve completely in water in the concentration range used in this research (from $1 \cdot 10^{-6}$ M to $1 \cdot 10^{-3}$ M).

Results and discussion

Synthesis of *p-tert*-butyl(thia)calix[4]arenes **1**, **2**

A large number of calixarenes functionalized with sulfonate groups at the upper rim have been recently received and used as self-assembled monolayers (Puplampu et al. 2015), components of porous materials (Aksoy et al. 2012; Han et al. 2009; Atwood et al. 2001; Atwood et al. 2004), and promoters of metallic catalysts (Komiyama et al. 1991). However, only few works are devoted to functionalization of the phenoxy fragments with tetraalkanesulfonate groups in case of the classic calixarene (Basilio et al. 2013; Gattuso et al. 2013). Thiacalixarenes with *O*-alkanesulfonate fragments at the lower rim are not known. Tetraalkylation of the lower rim (the phenol functions) is a standard method in the (thia)calix[4]arene skeleton modification (Iki et al. 1998; Iki et al. 1999; Kumar et al. 2014; Bhalla et al. 2004; Morohashi et al. 2006).

Calix[4]arene **1** (Fig. 1) was synthesized in a single step using previously reported procedure (Gattuso et al. 2013) by the reaction of *p-tert*-butylcalix[4]arene, 1,3-propanesultone, and NaH in refluxing anhydrous THF. In the classical calix[4]arene series, Na^+ in NaH should serve as an efficient template ion to yield *cone* conformers (Shinkai 1993) and the expected *cone* conformer **1** was yielded. The ^1H - ^1H NOESY NMR spectrum of the calix[4]arene **1** showed cross-peaks between (1) the aromatic protons of the macrocycle (6.67 ppm) and propylene protons (3.79, 2.85, 2.09 ppm) and (2) the *t*-butyl protons of the macrocycle (0.78 ppm) and propylene protons (3.79, 2.85, 2.09 ppm) (Fig. S5). It means that electrostatic repulsion of four charged substituents at the lower rim in the calix[4]arene **1** distorts the *cone* conformation, but nevertheless, there is no transition from the *cone* into *1,3-alternate* conformation.

The conformer distribution of alkylated thiacalix[4]arenes differs from that of classical calix[4]arenes and is governed by different metal template effects (Na^+ , K^+ , Cs^+) (Kumar et al. 2014). The presence of four sulfur atoms in thiacalix[4]arene

molecule imparts many novel features that govern significantly different behaviors and conformational preferences upon functionalization. Thiacalix[4]arene **2** was synthesized analogically to **1** in *cone* conformation instead of the expected *1,3-alternate* conformer using NaH/THF. The ^1H - ^1H NOESY NMR spectrum of the thiacalix[4]arene **2** does not have any cross-peaks between the aromatic and *t*-butyl protons of macrocycle and propylene protons of sulfonate fragments (Fig. S6). It is surprising that NaH/THF is suitable for the synthesis of the *cone* conformer because electrostatic repulsion of four negatively charged substituents at the lower rim in thiacalix[4]arene **2** should not have positioned it in the *cone* conformation as is observed in the synthesis of macrocycles with ester groups. Consequently, the *1,3-alternate* conformation of the product should have rather been expected. However, alkylation with *n*-PrI/NaH did not produce the expected *cone* conformation as with the classical calix[4]arene. The *cone* conformer of the tetraalkylated product of thiacalix[4]arene has been prepared using two-step dialkylation–dialkylation procedure in high yield (Himl et al. 2005). Consequently, the *cone* conformers in the thiacalixarene series bearing four alkyl groups at the lower rim are still hardly available for derivatization (Morohashi et al. 2000; Yamato et al. 2002). This is another example of how the conformational behavior of thiacalix[4]arenes differs from that of classical calix[4]arenes. Thus, we are the first to synthesize new tetrasubstituted thiacalix[4]arene with alkanesulfonate fragments at the lower rim in the *cone* conformation. The structure of the compounds obtained has been characterized by ^1H and ^{13}C , ^1H - ^1H NOESY NMR, IR spectroscopy, and mass spectrometry (ESI) (Figs. S1–S10).

Micelle formation of the compounds **1**, **2**

Synthesized macrocycles **1** and **2** are unique due to their supramolecular nature (host-guest complexes) and ability to form micelles (anionic surfactant). Micelle formation in colloidal solutions by surfactants is the most thermodynamically favorable process compared to processes whereby a solution or phase separation takes place. The aggregation mode of calixarene-based surfactants can be influenced by several factors, i.e., nature of the ionic groups, their position on the calixarene scaffold (upper or lower rim), the macrocycle size, and the length of the hydrophobic parts. (Thia)calix[4]arenes **1** and **2** contain long and bulky

hydrocarbon chains; critical micelle concentration (CMC) (concentration value above which micelles are formed) depends on their size and structure. Conductivity measurement and dynamic light scattering method were used to determine the CMC values. Conductivity determination of the CMC is based on the measurement of the concentration dependence of the electrical conductivity of ionic surfactant solutions. Conductivity measurements of macrocycles **1** and **2** solutions showed true solutions up to a concentration of $1.65 \cdot 10^{-5}$ M, followed by a sharp change in conductivity corresponding to the stage of micelles formation (Table S1). The CMC value for both macrocycles was similar to each other due to slight differences in their structure. Dynamic light scattering showed the presence of associates in solutions at the concentration of $1.65 \cdot 10^{-5}$ M. Note that a combination of the monomer analogs of calix[4]arenes (Yakimova et al. 2016b), sodium 3-phenylpropane-1-sulfonate and sodium 3-(4-(*tert*-butyl)phenoxy)propane-1-sulfonate, in the macrocycle decreases the CMC by tenfold (Table S2). However, the polydispersity index (PDI) for the solutions was quite high (PDI = 0.42 for the calixarene **1** and PDI = 0.57 for the thiacalixarene **2**). Obviously, it is possibly due to the following: (1) the bulky structure of the macrocycles with internal cavity, (2) the presence of four charged groups, and (3) the distorted *cone* conformation because of electrostatic repulsion of the charged sulfonate groups. These factors lead to the formation of micelles with different composition and form. The micelles can form associates with different size and shape. All this leads to an increase in the polydispersity of the system (Fig. 2).

Influence of these factors was confirmed by the DLS measurements of the self-association process for monomer analogs of calix[4]arenes (Yakimova et al. 2016b): sodium 3-phenylpropane-1-sulfonate and sodium 3-(4-(*tert*-butyl)phenoxy)propane-1-sulfonate. For sodium 3-phenylpropane-1-sulfonate, hydrodynamic diameter of the particles was 217.8 ± 23.4 nm (PDI = 0.42 ± 0.08) and for sodium 3-(4-(*tert*-butyl)phenoxy)propane-1-sulfonate 264.7 ± 31 nm (PDI = 0.43 ± 0.08) (Fig. S27, S29). In comparison, micelle diameter of the sodium dodecyl sulfate is near 3 nm (Cieřla et al. 2013). The polydisperse nanoparticles with different size and shape are present in the TEM image of the sample from the solutions of (thia)calix[4]arene (Fig. 2).

Self-assembled fractal hybrid dendrites in presence of Ag^+

To improve the monodispersity of the systems of macrocycles **1** and **2**, we propose the use of one of the most studied types of self-assembly based on spontaneous generation of certain metallosupramolecular architectures built from metal ions and organic ligands (Leninger et al. 2000; Lawrence et al. 1995; MacGillivray and Atwood 1999; Fujita et al. 2005). Organic compounds in such structures should possess molecular recognition ability for certain types of substrates and provide the necessary spatial structural arrangement for binding sites and functional groups. In this case, metal ions act as coordinating centers directing the organic ligands in a certain way. In addition, metal ions ensure the reversibility of association-dissociation of supramolecular assemblies, and thus, they are the switchable centers of the interactions. This combination of the above properties allows preparing supramolecular structures with a high degree of symmetry (Poole and Owens 2003). Modification of the macrocyclic platform by appropriate reagents for providing desired orientation of the binding centers in space for selective interaction with a substrate is one of the most successful approaches employed in the creation of such receptors (Atwood et al. 1996). The diversity of supramolecular structures is determined by the ability of receptors with various heteroatoms (S, N, O) with lone pairs to bind metal cations via donor-acceptor interactions outside the cavity of the macrocycle. The structure of *p-tert*-butylthiacalix[4]arenes (nature of the binding sites and conformation of macrocycle) and the preferred coordination geometry of metal ions, which define the relative positioning of macrocycles in space and the shape of particle, are the limiting factors of the exo-recognition process. Calix[4]arene **1** and thiacalix[4]arene **2** molecules are of great interest as components for self-assembled architectures because their structures contain potential coordination centers for metal cations (bridged sulfur atoms and negatively charged sulfonate groups) (Fig. 1). Treatment of the colloidal solutions of the macrocycles ($c = 10^{-4}$ M) with one equivalent of silver nitrate led to the spontaneous self-assembly of the macrocycles. Dynamic light scattering method showed an increasing monodispersity and monomodal size distribution by intensity (Fig. 2). For calix[4]arene **1**, hydrodynamic diameter of the particles is 211.1 ± 11.6 nm (PDI = 0.412 ± 0.01), and for the thiacalix[4]arene **2** is

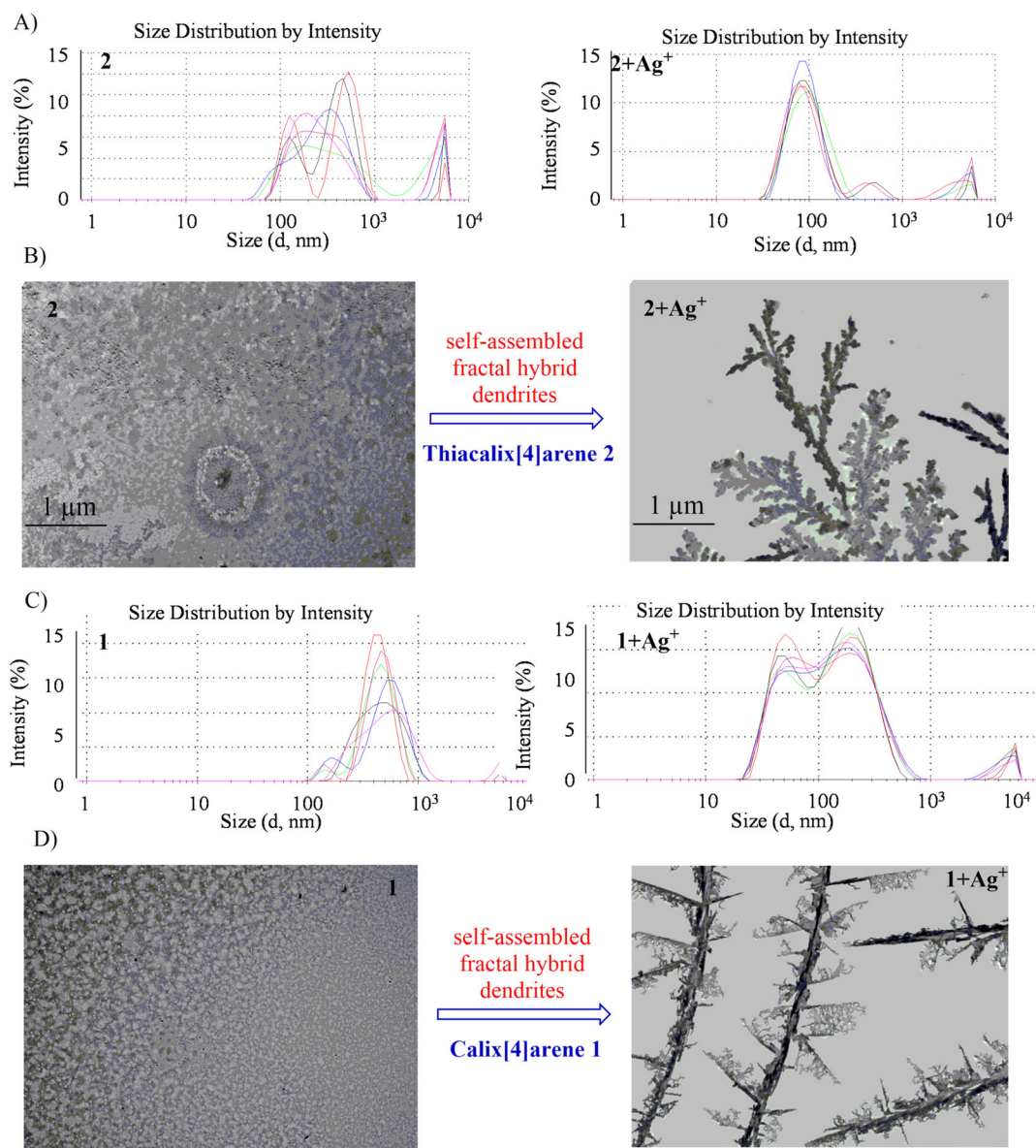


Fig. 2 a (at the left) Size distribution of the particles by intensity for macrocycle **2** solution ($1 \cdot 10^{-4}$ M); (from the right) size distribution of the particles by intensity for macrocycle **2** solution ($1 \cdot 10^{-4}$ M) + AgNO_3 ($1 \cdot 10^{-4}$ M) with a mol ratio 1:1 in water. b (at the left) TEM images of macrocycle **2** after the solvent evaporation; (from the right) TEM images of the Ag-based aggregates **2** (macrocycle **2** + AgNO_3 after solvent evaporation). c (at the left)

Size distribution of the particles by intensity for macrocycle **1** solution ($1 \cdot 10^{-4}$ M); (from the right) Size distribution of the particles by intensity for macrocycle **1** solution ($1 \cdot 10^{-4}$ M) + AgNO_3 ($1 \cdot 10^{-4}$ M) with a mol ratio 1:1 in water. d (at the left) TEM images of macrocycle **1** after the solvent evaporation; (from the right) TEM images of Ag-based aggregates **1** (macrocycle **1** + AgNO_3 after the solvent evaporation)

94.6 ± 7 nm (PDI = 0.23 ± 0.01). It is evident that the presence of the bridged sulfur atoms in the macrocycle structure leads to a decrease in the polydispersity index. It is obvious that the replacement of methylene bridged fragments in calix[4]arene structure by sulfur bridges in thiacalix[4]arene leads to the formation of S-Ag-S

bonds, not typical for classical calixarenes. Note that addition of AgNO_3 to monomer analogs of **1** and **2** leads to a minor decrease in diameter of the associates to 201.3 ± 14.5 nm (sodium 3-phenylpropane-1-sulfonate) and 153.2 ± 6.4 nm (sodium 3-(4-(*tert*-butyl)phenoxy)propane-1-sulfonate), correspondingly,

and an increase in monodispersity to PDI = 0.35 (Figs. S28, S30). Consequently, the more dense packing of macromolecules and their reduced size and polydispersity are caused by the formation of S–Ag–S bonds.

TEM analysis of fractal hybrid dendrites formed from Ag-based aggregates

In order to confirm the formation of the supramolecular Ag-based aggregates formed by *p*-tert-butyl(thia)calix[4]arenes with silver ions, colloidal systems of compounds **1** and **2** with AgNO₃ were studied by TEM. Samples were prepared by solvent evaporation on air. The TEM shows the morphology of the structures formed (Fig. 2b, d). According to the images obtained after the evaporation of the solvent from the particles, dendrite fractal structures were formed in both cases. This can be explained by the formation of supramolecular associates of the (thia)calix[4]arene and silver ions. Because of the high affinity of the macrocycles to sulfur atoms resulting from the donor-acceptor bonds, aggregates form after evaporation of solvent and they further associate with non-covalently bonded clusters of colloid particles leading to the formation of dendrite fractal structures of Ag-based aggregates. For characterization of dendrite fractal structures formed by calix[4]arene **1**

and thiacalix[4]arene **2**, we used the most common mode of the TEM operation, i.e., the bright field imaging mode. In this mode, the contrast formation, when considered classically, is formed directly by occlusion and absorption of the electrons in the sample. Therefore, regions of the sample with a higher atomic number appear dark, while regions with no sample or regions with lower atomic number in the beam path appear bright.

Analyzing the two types of dendrite fractal structures, it is possible to conclude that the principles defining their formation are different. The bridged sulfur in thiacalixarene **2** plays a decisive role in the formation of spherical Ag-based aggregates and the fractal structures. The Ag-based aggregates, in turn, are transformed in the structure presented in Fig. 2b (from the right). This is evident due to the uniform distribution of light (the atoms in macrocycle structure) and dark (silver ions) regions in such a structure. In the case of the dendritic structures of calixarene **1** and silver nitrate, the visible dark skeleton (silver with higher atomic number) clearly appears. Along this core, lighter regions are related to the calixarene molecules **1**. Distribution of heavier and lighter atoms is unequal indicating a different mechanism for the formation of the fractal structure. Here, sulfonate fragments, which participates in the formation of the

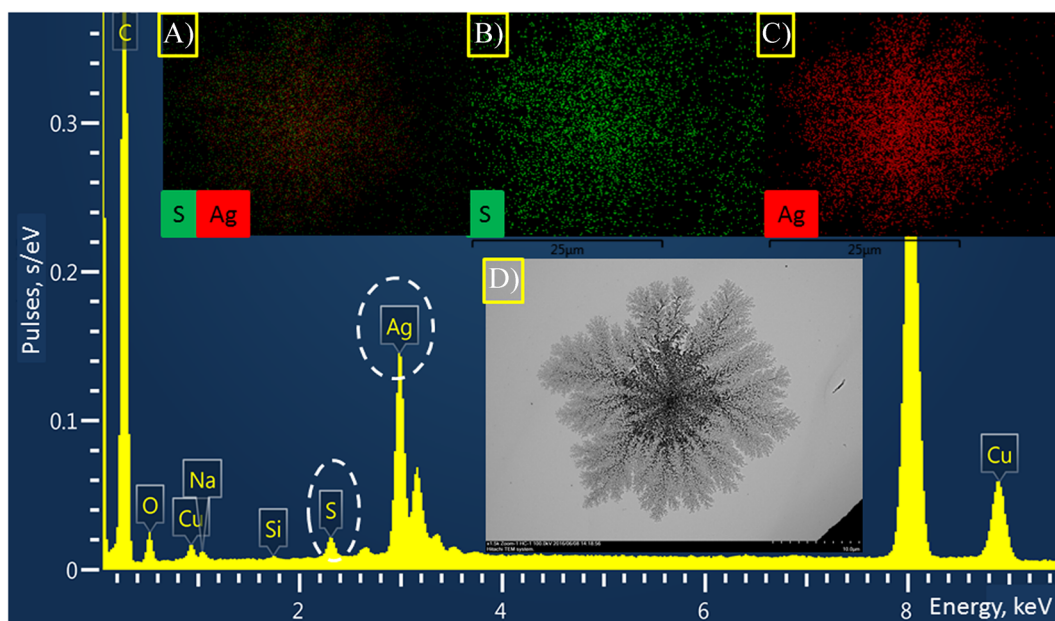


Fig. 3 Energy-dispersion spectrum of fractal dendrite structure formed thiacalix[4]arene **2** and Ag⁺ on the copper support. On the insert **a**: superposition of elemental maps of S and Ag in the fractal

dendrite structure formed by thiacalix[4]arene **2** and Ag⁺. **b** Mapping of S. **c** Mapping of Ag. **d** Fractal dendrite structure formed by thiacalix[4]arene **2** and Ag⁺

donor-acceptor bonds O–Ag, play a decisive role. Most molecules of the calixarene **1** are oriented along the silver core.

Elemental maps of a fractal dendrite structure

Representative elemental maps of the fractal dendrite structure formed by the thiacalix[4]arene **2** and Ag⁺ on the FormvarTM/carbon coated 3 mm copper grid are shown in Fig. 3. Maps from full fractal dendrite structure were acquired to confirm that these images were representative for the sample. The boxed region in the image (Fig. 3a–c) shows the region over which the elemental maps were acquired. Elemental maps for S and Ag (Fig. 3b, c, respectively) clearly reveal their locations in the dendrite. By comparing spatial features in both the Ag and S maps, it seems that there is a certain degree of correlation between the locations of these two elements because the regions of higher Ag intensity appear at regions of higher S intensity. Two maps are not identical though, and Ag looks to be dispersed over the support more than sulfur, which has been speculated to occur in a related Ag–S dendrite structure. We note that the synthesized Ag-based aggregate solutions are stable for a sufficiently long time (not less than 30 days). Constant hydrodynamic diameter of Ag-based aggregates is confirmed by dynamic light scattering.

Conclusion

In conclusion, we have synthesized the first water-soluble thiacalix[4]arene bearing *O*-propanesulfonato groups at the lower rim and studied its self-assembly in aqueous solution. We showed that tetrasubstituted thiacalix[4]arene with *O*-propanesulfonate fragments at the lower rim exists in the *cone* conformation but not the expected *1,3-alternate*. A simple approach for the design of stable monodisperse Ag-based aggregates with organic ligands has been realized in water by the addition of AgNO₃ solution: hydrodynamic diameter of the thiacalix[4]arene associates is about 95 nm with low PDI. Self-assembled fractal hybrid nanodendrites from water-soluble anionic (thia)calix[4]arenes and Ag⁺ have been designed.

Our method provides a facile single-step approach for the fast preparation of complex dendritic Ag nanostructures at room temperature. Such dendritic structures

have intricate structural characteristics and, therefore, are touted to be highly favored structures for the preparation of advanced nanodevices.

Acknowledgments This publication was supported by the Ministry of Education and Science of the Russian Federation (the Agreement number 02.a03.21.0008), the Russian Foundation for Basic Research (grant. no. 15-03-02877) and the research grant of Kazan Federal University.

Compliance with ethical standards

Conflict of interest The authors declare that they have no conflict of interest.

References

- Aksoy T, Erdemir S, Yildiz HB, Yilmaz M (2012) Novel water-soluble calix[4,6]arene appended magnetic nanoparticles for the removal of the carcinogenic aromatic amines. *Water Air Soil Pollut* 223:4129–4139. doi:10.1007/s11270-012-1179-4
- Ariga K, Ito H, Hill JP, Tsukube H (2012) Molecular recognition: from solution science to nano/materials technology. *Chem Soc Rev* 35:5800–5835. doi:10.1039/C2CS35162E
- Ariga K, Ji Q, Mori T, Naito M, Yamauchi Y, Abe H, Hill JP (2013) Enzyme nanoarchitectonics: organization and device application. *Chem Soc Rev* 42:6322–6345. doi:10.1039/C2CS35475F
- Atwood JL, Steed JW (2008) *Organic Nanostructures*. Wiley-VCH, Weinheim
- Atwood JL, Davies JED, MacNicol DD, Vogtle F, Lehn J-M (1996) *Comprehensive in comprehensive supramolecular chemistry*. Pergamon Press, Oxford
- Atwood JL, Barbour LJ, Hardie MJ, Raston CL (2001) Metal sulfonatocalix[4,5]arene complexes: bi-layers, capsules, spheres, tubular arrays and beyond. *Coord Chem Rev* 222(1):3–32. doi:10.1016/S0010-8545(01)00345-9
- Atwood JL, Dalgarno SJ, Hardie MJ, Raston CL (2004) Hydrogen-bonded arrays of a ytterbium(III) p-sulfonatocalix[6]arene complex. *New J Chem* 28(2):326–328. doi:10.1039/B311288H
- Basilio N, Francisco V, Garcia-Rio L (2013) Aggregation of *p*-Sulfonatocalixarene-based Amphiphiles and supra-Amphiphiles. *Int J Mol Sci* 14:3140–3157. doi:10.3390/ijms14023140
- Bhalla V, Kumar M, Hattori T, Miyano S (2004) Stereoselective synthesis of all stereoisomers of vicinal and distal bis(O-2-aminoethyl)-*p*-tert-butylthiacalix[4]arene. *Tetrahedron* 60(28):5881–5887. doi:10.1016/j.tet.2004.05.035
- Boal AK, Ilhan F, DeRouchey JE, Thurn-Albrecht T, Russell TP, Rotello VM (2000) Self-assembly of nanoparticles into structured spherical and network aggregates. *Nature* 404:746–748. doi:10.1038/35008037
- Chen N, Zheng Y, Yin J, Li X, Zheng CJ (2013) Inhibitory effects of silver nanoparticles against adenovirus type 3 in vitro.

- Viol Methods 193:470–477. doi:10.1016/j.jviromet.2013.07.020
- Cieřla J, Bieganowski A, Narkiewicz-Michalek J, Szymula M (2013) Use of a dynamic light scattering technique for SDS/water/Pentanol studies. *J Disper Sci Technol* 34:566–574. doi:10.1080/01932691.2012.680834
- Fujita M (2000) Molecular self-assembly organic versus inorganic approaches. Springer-Verlag, Berlin
- Fujita M, Tominaga M, Therrien B (2005) Coordination assemblies from a Pd(II)-cornered square complex. *Acc Chem Res* 38(4):369–378. doi:10.1021/ar040153h.1021/ar040153h
- Galdiero S, Falanga A, Vitiello M, Cantisani M, Marra V, Galdiero M (2011) Silver nanoparticles as potential antiviral agents. *Molecules* 16:8894–8918. doi:10.3390/molecules16108894
- Gattuso G, Notti A, Pappalardo A, Pappalardo S, Parisi MF, Puntoriero F (2013) A supramolecular amphiphile from a new water-soluble calix[5]arene and n-dodecylammonium chloride. *Tetrahedron Lett* 54:188–191. doi:10.1016/j.tetlet.2012.10.125
- Gorbachuk VV, Ziganshin MA, Savelyeva LS, Mironov NA, Habicher WD (2004) Cooperative hydration effect on the binding of organic vapors by a cross-linked polymer and beta-cyclodextrin. *Macromol Symp* 210:263–270. doi:10.1002/masy.200450630
- Han C, Zeng L, Li H, Xie G (2009) Colorimetric detection of pollutant aromatic amines isomers with *p*-sulfonatocalix[6]arene-modified gold nanoparticles. *Sensor Actuat B-Chem* 137:704–709. doi:10.1007/s11051-014-2585-x
- Himl M, Pojarova M, Stibor I, Sykora J, Lhotak P (2005) Stereoselective alkylation of thiacalix[4]arenes. *Tetrahedron Lett* 46:461–464. doi:10.1016/j.tetlet.2004.11.077
- Hussain I, Brust M, Papworth AJ, Cooper AI (2003) Preparation of acrylate-stabilized gold and silver hydrosols and gold-polymer composite films. *Langmuir* 19:4831–4835. doi:10.1021/la020710d
- Iki N, Narumi F, Fujimoto T, Morohashi N, Miyano S (1998) Stereocontrolled oxidation of a thiacalix[4]arene to the sulfanyl counterpart of a defined SO configuration. *J Chem Soc Perkin Trans* 12:2745–2750. doi:10.1039/A803734E
- Iki N, Morohashi N, Narumi F, Fujimoto T, Suzuki T, Miyano S (1999) Novel molecular receptors based on a thiacalix[4]arene platform. Preparation of di- and tetracarboxylic acid derivatives and their binding properties towards transition metal ions. *Tetrahedron Lett* 40(41):7337–7341. doi:10.1016/S0040-4039(99)01503-8
- Komiyama M, Isaka K, Shinkai S (1991) Water-soluble calixarene as the first man-made catalyst for regioselective cleavage of ribonucleoside 2',3'-cyclic phosphate. *Chem Lett*:937–940. doi:10.1246/cl.1991.937
- Kumar R, Lee YO, Bhalla V, Kumar M, Kim JS (2014) Recent developments of thiacalixarene based molecular motifs. *Chem Soc Rev* 43:4824–4870. doi:10.1039/C4CS00068D
- Landsdown AB (2010) Silver in healthcare: its antimicrobial efficacy and safety in use. Royal Society of Chemistry, Cambridge
- Lawrence DS, Jiang T, Levett M (1995) Self-assembling supramolecular complexes. *Chem Rev* 95(6):2229–2260. doi:10.1021/cr00038a018
- Leninger S, Olenyuk B, Stang P (2000) Self-assembly of discrete cyclic nanostructures mediated by transition metals. *J Chem Rev* 100(3):853–908. doi:10.1021/cr9601324
- Lindoy LF, Atkinson IM (2000) Self assembly in supramolecular systems. Royal Society of Chemistry, Cambridge, UK
- MacGillivray LR, Atwood JL (1999) Structural classification and general principles for the design of spherical molecular hosts. *Angew Chem Int Ed* 38(8):1018–1033. doi:10.1023/A:1014540609454
- Melnikau D, Savateeva D, Lesnyak V, Gaponik N, Nunez Fernández Y, Vasilevskiy MI, Costa MF, Mochalov KE, Oleinikov V, Rakovich YP (2013) Resonance energy transfer in self-organized organic/inorganic dendrite structures. *Nano* 5:9317–9323. doi:10.1021/cg201351j
- Mohammed FA, Ao Z, Girilal M, Chen L, Xiao X, Kalaichelvan P, Yao X (2012) Inactivation of microbial infectiousness by silver nanoparticles-coated condom: a new approach to inhibit HIV- and HSV-transmitted infection. *Int J Nanomedicine* 7:5007–5018. doi:10.2147/IJN.S34973
- Mohanty A, Garg N, Jin RC (2010) A universal approach to the synthesis of noble metal nanodendrites and their catalytic properties. *Angew Chem Int Ed* 49:4962–4966. doi:10.1002/anie.201000902
- Morohashi N, Iki N, Kabuto C, Miyano S (2000) Stereocontrolled oxidation of a thiacalix[4]arene to the sulfanyl counterpart of a defined SO configuration. *Tetrahedron Lett* 41:2933–2937. doi:10.1016/S0040-4039(00)00313-0
- Morohashi N, Narumi F, Iki N, Hattori T, Miyano S (2006) Thiacalixarenes. *Chem Rev* 106(12):5291–5316. doi:10.1021/cr050565j
- Polshettiwar V, Baruwati B, Varma RS (2009) Self-assembly of metal oxides into three-dimensional nanostructures: synthesis and application in catalysis. *ACS Nano* 3:728–736. doi:10.1021/nn800903p
- Poole CP Jr, Owens FJ (2003) Introduction to nanotechnology. Wiley, Hoboken
- Puplampu JB, Yakimova LS, Vavilova AA, Fayzullin DA, Zuev YF, Stoikov II (2014) Synthesis of *p*-tert-butylthiacalix[4]arenes functionalized with tris(2-aminoethyl)amine fragments at the lower rim and their interaction with model lipid membranes. *Macrocyclics* 7(4):337–344. doi:10.6060/mhc140489s
- Puplampu JB, Yakimova LS, Vavilova AA, Rizvanov IK, Stoikov II (2015) *P*-tert-butyl Thiacalix[4]arene derivatives functionalized in the lower rim with Bis(3-aminopropyl)amine: synthesis and interaction with DNA. *Macrocyclics* 8(1):75–80. doi:10.6060/mhc140722s
- Shinkai S (1993) Calixarenes - the third generation of supramolecules. *Tetrahedron* 49(40):8933–8968. doi:10.1016/S0040-4020(01)91215-3
- Shurpik DN, Yakimova LS, Makhmutova LI, Makhmutova AR, Rizvanov IK, Plemenkov VV, Stoikov II (2014) Pillar[5]arenes with morpholide and pyrrolidide substituents: synthesis and complex formation with alkali metal ions. *Macrocyclics* 7(4):351–357. doi:10.6060/mhc140719s
- Shurpik DN, Padnya PL, Makhmutova LI, Yakimova LS, Stoikov II (2015a) Selective stepwise oxidation of 1,4-decamethoxypillar[5]arene. *New J Chem* 39(12):9215–9220. doi:10.1039/C5NJ01951F
- Shurpik DN, Yakimova LS, Rizvanov IK, Plemenkov VV, Stoikov II (2015b) Water-soluble pillar[5]arenes: synthesis and characterization of the inclusion complexes with *p*-

- toluenesulfonic acid. *Macroheterocycles* 8(2):128–134. doi:10.6060/mhc140928s
- Steed JW, Atwood JL (2009) *Supramolecular chemistry*, 2nd edn. John Wiley, New York
- Stoikov II, Mostovaya OA, Yakimova LS, Yantemirova AA, Antipin IS, Konovalov AI (2010) Phosphorus-bridged calixarene phosphites: dramatic influence of a tert-butyl group at the upper rim of the macrocycle upon anion binding. *Mendeleev Commun* 20(6): 359–360. doi:10.1016/j.mencom.2010.11.021
- Vavilova AA, Nosov RV, Yakimova LS, Antipin IS, Stoikov II (2013) Synthesis of photo-switchable derivatives of *p-tert-butyl* Thiocalix[4]arenes containing Ethoxycarbonyl and 4-Amidoazobenzene fragments in the lower rim substituents. *Macroheterocycles* 6(3): 219–226. doi:10.6060/mhc130748s
- Wen XG, Xie YT, Mak MWC, Cheung KY, Li XY, Renneberg R, Yang SH (2006) Dendritic nanostructures of silver: facile synthesis, structural characterizations, and sensing applications. *Langmuir* 22:4836–4842. doi:10.1021/la060267x
- Witten TA, Sander LM, (1981) Diffusion-limited aggregation, a kinetic critical phenomenon. *Phys rev Lett* 47:1400–1403. doi: 10.1103/PhysRevLett.47.1400
- Yakimova LS, Shurpik DN, Stoikov II (2016a) Amide-functionalized pillar[5]arenes as a novel class of macrocyclic receptors for the sensing of H₂PO₄⁻ anion. *Chem Commun* 52(84):12462–12465. doi:10.1039/C6CC05797G
- Yakimova LS, Shurpik DN, Gilmanova LH, Makhmutova AR, Rakhimbekova A, Stoikov II (2016b) Highly selective binding of methyl orange dye by cationic water-soluble pillar[5]arenes. *Org Biomol Chem* 14:4233–4238. doi:10.1039/C6OB00539J
- Yamato T, Zhang F, Kumamaru K, Yamamoto H (2002) Synthesis, conformational studies and inclusion properties of Tetrakis[(2-pyridylmethyl)oxy]thiocalix[4]arenes. *J Incl Phenom Macro Chem* 42:51–60. doi:10.1023/A:1014540609454
- Zhou P, Dai ZH, Fang M, Huang XH, Bao JC (2007) Novel dendritic palladium nanostructure and its application in Biosensing. *J Phys Chem C* 111:12609–12616. doi:10.1021/jp072898l
- Ziganshin MA, Yakimova LS, Khayarov KR, Gorbachuk VV, Vysotsky MO, Böhmer V (2006) Guest exchange in dimeric capsules of a tetraurea calix[4]arene in the solid state. *Chem Commun* 37:3897–3899. doi:10.1039/b607568a